




Water aging and the quality of organic carbon sources drive niche partitioning of the active bathypelagic prokaryotic microbiome

Marta Sebastián ^{1*}, Pablo Sánchez,¹ Guillem Salazar,² Xosé A. Álvarez-Salgado,³ Isabel Reche ⁴,
Xosé Anxelu G. Morán ⁵, Maria Montserrat Sala,¹ Carlos M. Duarte,⁶ Silvia G. Acinas,¹ Josep M. Gasol¹

¹Department of Marine Biology and Oceanography, Institut de Ciències del Mar, CSIC, Barcelona, Catalunya, Spain

²Department of Biology, Institute of Microbiology and Swiss Institute of Bioinformatics, ETH Zurich, Zürich, Switzerland

³Instituto de Investigaciones Mariñas (IIM-CSIC), Vigo, Galicia, Spain

⁴Departamento de Ecología and Research Unit Modeling Nature (MNat), Universidad de Granada, Granada, Spain

⁵Centro Oceanográfico de Gijón/Xixón, IEO, CSIC, Gijón/Xixón, Asturias, Spain

⁶Red Sea Research Centre (RSRC), King Abdullah University of Science and Technology, Thuwal, Saudi Arabia

Abstract

Due to the scarcity of organic matter (OM) sources in the bathypelagic (1000–4000 m depth), prokaryotic metabolism is believed to be concentrated on particles originating from the surface. However, the structure of active bathypelagic prokaryotic communities and how it changes across environmental gradients remains unexplored. Using a combination of 16S rRNA gene and transcripts sequencing, metagenomics, and substrate uptake potential measurements, here we aimed to explore how water masses aging and the quality of OM influence the structure of the active microbiome, and the potential implications for community function. We found that the relative contribution of taxa with a free-living lifestyle to the active microbiome increased in older water masses that were enriched in recalcitrant OM, suggesting that these prokaryotes may also play a substantial role in the bathypelagic metabolism of vast areas of the ocean. In comparison to particle-associated prokaryotes, free-living prokaryotes exhibited lower potential metabolic rates, and harbored a limited number of two-component sensory systems, suggesting they have less ability to sense and respond to environmental cues. In contrast, particle-associated prokaryotes carried genes for particle colonization and carbohydrate utilization that were absent in prokaryotes with a free-living lifestyle. Consistently, we observed that prokaryotic communities inhabiting older waters displayed reduced abilities to colonize particles, and higher capabilities to use complex carbon sources, compared to communities in waters with a higher proportion of labile OM. Our results provide evidence of regionalization of the bathypelagic active prokaryotic microbiome, unveiling a niche partitioning based on the quality of OM.

*Correspondence: msebastian@icm.csic.es

This is an open access article under the terms of the [Creative Commons Attribution-NonCommercial](https://creativecommons.org/licenses/by-nc/4.0/) License, which permits use, distribution and reproduction in any medium, provided the original work is properly cited and is not used for commercial purposes.

Additional Supporting Information may be found in the online version of this article.

Author Contribution Statement: GS contributed to the collection of microbial samples. MS performed RNA extractions. GS and MS performed the sequence data processing and the statistical analyses. CMD led the Malaspina 2010 Expedition and JMG led the microbial block of the expedition and both provided the ancillary data. SGA obtained the JGI grant that made possible the sequencing of the DNA and RNA samples. PS helped with the bioinformatics work. MMS provided the BIOLOG data and IR and XAAS provided the FDOM data. JMG and XAGM provided prokaryotic specific growth rates. MS conceived and wrote the paper. All authors contributed to the final version of the paper.

The bathypelagic ocean (1000–4000 m) contains ca. 35% of the ocean's prokaryotes (bacteria and archaea) (Aristegui et al. 2009), but many aspects of their ecology and niche partitioning remain mostly unexplored. Due to the scarcity and recalcitrant nature of the dissolved organic carbon in this ecosystem (Hansell et al. 2009), the energy needs of bathypelagic prokaryotes are mostly met by pulses of labile carbon introduced via surface-derived sinking particles (Smith et al. 2018) or actively transported by zooplankton and vertebrates (Hernández-León et al. 2020). Considering that most organic matter (OM) exported from the photic layer is remineralized within the mesopelagic (Aristegui et al. 2005), and given the extreme environmental conditions characterized by low temperature and high pressure typical of the bathypelagic, the activity of deep ocean prokaryotes was traditionally assumed to be very low. However, this view was challenged by the observation of relatively high respiration and exoenzyme

activity rates in deep waters (Baltar et al. 2009b). Suspended particles of unknown origin (Baltar et al. 2009a) or in situ chemolithoautotrophy (Reinthal et al. 2010) may also be significant carbon sources for bathypelagic metabolism, and thus, the regulation of the activity of deep ocean prokaryotes may be more complex than previously believed.

Initial metagenomic studies suggested that most prokaryotes in bathypelagic waters have a particle-associated lifestyle (DeLong et al. 2006). This view is supported by recent findings using combined -omics approaches hinting that most of the bathypelagic heterotrophic metabolic activity is mediated by particle-associated prokaryotes (Bergauer et al. 2018; Zhao et al. 2020). However, particle-associated prokaryotes represent only a minor fraction (~10%) of bathypelagic communities (Mével et al. 2008; Zhang et al. 2020), and there is experimental evidence that bathypelagic prokaryotic communities are very resilient to the long-term absence of external sources of carbon (Sebastián et al. 2018, 2019). These findings, together with observations of potential metabolic versatility in single-amplified-genomes of deep ocean prokaryotes (Swan et al. 2011; Tang et al. 2016; Landry et al. 2017) and in metagenome-assembled genomes reconstructed from the global bathypelagic (Acinas et al. 2021), suggest that in the absence of particles or in periods of low particle flux, bathypelagic metabolism may be sustained by free-living communities.

DNA-based surveys have shown that particle-associated and free-living communities in the bathypelagic differ in many dominant phyla and/or classes (Salazar et al. 2015), suggesting that these two lifestyles have been strongly conserved through their evolutionary history. A recent study indeed showed differences in key metabolic genes of bathypelagic free-living and particle-associated communities using size-fractionated metagenomes (Acinas et al. 2021). However, particle-associated taxa may also be released in bathypelagic waters upon detachment from particles (Sohrin et al. 2011), and even thrive in those deep waters receiving elevated particle flux, in which the OM quality is higher.

The optical properties of dissolved organic matter (DOM) can serve as tracers for both ocean circulation and of biochemical processes (Nelson and Siegel 2013). For example, protein-like fluorescence is linked to primary productivity (Jørgensen et al. 2011; Carr et al. 2019), and its presence in the bathypelagic likely reflects fresh labile carbon inputs. Conversely, humic-like fluorescence is indicative of by-products resulting from microbial respiration, which have comparatively longer turnover times and accumulate following water mass aging (Yamashita and Tanoue 2008; Jørgensen et al. 2011; Catalá et al. 2015b). Using parallel factor analysis (PARAFAC), four fluorescent components have been identified to be ubiquitous and common in the dark global ocean (Yamashita and Tanoue 2008; Jørgensen et al. 2011; Catalá et al. 2015b), two humic-like components and two protein-like components (Catalá et al. 2015b). The contribution of these components to DOM fluorescence recently emerged as one of the main drivers of the taxonomic composition of both free-living and particle-associated bathypelagic

communities from eight ocean stations broadly distributed (Ruiz-González et al. 2020). In addition, it has been shown that water masses influence the structure of both free-living and particle-associated bathypelagic communities (Salazar et al. 2016). This structuring role may be reflecting changes in the quality of the organic resources of each water mass, but this has never been investigated at the global scale.

Here, we explored the role of water masses aging and associated changes in the quality of organic resources in driving the assembly of the active bathypelagic prokaryotic microbiome using 16S rRNA transcripts (abbreviated herein as RNA) from 30 stations sampled in the global tropical and subtropical ocean. The quality of OM was addressed through the optical properties of its fluorescent fraction, using the ratio between the protein-like (i.e., putatively more labile) and humic-like (i.e., putatively more recalcitrant) components mentioned above. We assessed the niche partitioning of different prokaryotic families, and showed there is a clear segregation based on the OM quality and water mass aging. The contribution of different lifestyles (free-living, dual, and particle-associated) to the total and active prokaryotic free-living microbiome also varied remarkably following changes in the OM quality. Using published metagenomes from these same stations we delineated the functional repertoire of free-living and particle-associated prokaryotes using a differential abundance (DA) approach and explored how these functions vary in waters with contrasting OM lability. The substrate use capabilities of these communities was further explored using Biologs GN2 plates. Given that the nature of the OM is likely a selecting pressure for different prokaryotic lifestyles in the bathypelagic, we hypothesized that there is a functional regionalization of the bathypelagic microbiome, with varying contribution of lifestyles depending on the quality of the OM.

Materials and methods

A total of 101 water samples were collected during the Malaspina 2010 expedition corresponding to 30 different sampling stations globally distributed across the subtropical and tropical region of the world's oceans between 2150 and 4000 m depth (median depth: 4000 m; Supplementary Table S1; Fig. S1). Samples were obtained for 16S rRNA genes (hereafter referred as DNA) and 16S rRNA transcripts (hereafter referred as RNA) sequencing of communities from the 0.2–0.8 and the 0.8–20 μm size fraction to discern typical free-living communities from particle-associated ones (see Supplementary methods for methodological considerations).

The 16S DNA samples were reported before (Salazar et al. 2015, 2016) and consist of 60 samples from 30 different stations for which both size fractions are available (Supplementary Fig. S1). The 16S RNA dataset is new and it consists of 41 samples (27 from the 0.2–0.8 μm size fraction and 14 from the 0.8–20 μm size fraction, Fig. S1). In this study, we only used the 16S DNA samples for the delineation

of the different lifestyles (see explanation below) and to assess the RNA : DNA relationships of the different lifestyles. Details on sample collection, and nucleic acids extraction, sample and sequencing processing can be found in the Supplementary Methods. Exact amplicon sequence variants (ASVs) were obtained with DADA2 v1.8 (Callahan et al. 2016).

Given the large difference in the sequencing effort for the 16S DNA and the RNA pool (Supplementary Table S1), for downstream analyses the ASV table was sampled down to the minimum number of reads (17,824 reads/sample) to avoid artifacts due to the uneven sequencing effort among samples, using the *rarefy* function in the *vegan* package. This process was repeated 100 times and the mean number of reads (rounded to integers) from the 100 rarefactions was used.

Drivers of the active prokaryotic microbiome

Nonmetric multidimensional scaling (NMDS, *metaMDS* function, R Vegan package, Oksanen et al., 2015) was used to visualize spatial differences between samples based on Bray-Curtis distances of the rarefied ASV abundance table from the 16S RNA pool. A description of downstream analyses to assess the environmental drivers of the active community structuring can be found in the Supplementary methods.

Categorization of ASVs in the different lifestyle categories

To categorize ASVs into different lifestyles we used a differential abundance (DA) approach (see Supplementary methods for further details on why we chose this approach). The analysis was performed on 16S DNA sequences because the amount of ribosomes and transcriptional activity vary strongly among prokaryotes (Cottrell and Kirchman 2016), and copiotrophic taxa containing a large number of ribosomes could mask the 16S RNA sequences of slow growers. The DA analysis was performed using the *Corncob* package (v. 0.1.0) (Martin et al. 2020). This approach differs from the one used in the previous paper with the same 16S DNA dataset to delineate prokaryotes with a FL and PA lifestyle (Salazar et al. 2015) because here the analysis was done with ASVs instead of 97% OTUs, and *Corncob* was chosen because it takes into account the complexity of compositional data. Wald tests with a false discovery rate threshold of 0.05 were applied. Those ASVs predominantly found in the 0.2–0.8 μm size fraction were categorized as having a “free-living lifestyle” (FL-ls). ASVs that did not have significant differences in their distributions in both size-fractions were categorized as “dual lifestyle” (dual-ls), and those ASVs predominantly found in the 0.8–20 μm size fraction were considered as ASVs with a “particle-associated lifestyle” (PA-ls). The dual-ls category could be due to methodological biases related to the size-fractionation approach employed, but also to the existence of a dual-ls group of organisms, that is, prokaryotes that thrive on particles but may withstand long periods of time in the free-living realm, between successful encounters with particles. In addition, there were 627 rare ASVs for which we were not able to fit the beta-

binomial model (representing only from 0.08% to 5% of the reads, median 0.4%).

All data treatment and statistical analyses were conducted with the R Statistical Software using version 3.2.4.

Characterization of OM resources

As mentioned above, OM was characterized through the optical properties of its fluorescent fraction, which provide information about the origin and lability of organic resources. Four main fluorescence components (C1–C4) were recovered from the excitation-emission matrices using PARAFAC (see Catalá et al. 2015b for further details). The percentage contribution of each component (relative to the summed maximum fluorescence of the four PARAFAC components) was computed to characterize the fluorescent DOM (FDOM) as in (Ruiz-González et al. 2020). The protein-like components C3 and C4 have been attributed to tryptophan and tyrosine, respectively (Catalá et al. 2015b). A good correlation between the tryptophan-like FDOM component and the carbon (carbohydrates) and nitrogen (amino acids) content of semi-labile DOM was recently found (Devresse et al. 2023), supporting the use of FDOM properties to trace the lability of OM. In addition, there is a tight covariation of the two labile C3 and C4 FDOM components between surface and bathypelagic waters (Ruiz-González et al. 2020), suggesting that sinking particles arriving to the deep ocean release these components. Conversely, C1 and C2 are attributed to recalcitrant by-products of microbial respiration (Yamashita and Tanoue 2008; Jørgensen et al. 2011; Catalá et al. 2015b), which includes both free-living and particle-associated prokaryotes. It has been reported that the less labile the OM substrates are, the largest is the amount of recalcitrant FDOM produced relative to the carbon that is remineralized (Jørgensen et al. 2014). Thus, the proportion of labile (C3 + C4) to recalcitrant (C1 + C2) FDOM components was used here as a proxy for the relative lability (or quality) of the OM landscape (i.e., in both the dissolved and particulate phases, as more labile material likely reflects the presence of fresher particles that are releasing these compounds).

Links between prokaryotic taxa and biotic and abiotic variables

The association of the representation of different prokaryotic families in the RNA pool with the quality of OM and other biotic and abiotic variables were explored using a Sparse partial least squares (sPLS) regression analysis (see Supplementary methods for further details).

Links between the assembly of the active prokaryotic microbiome and OM quality and other environmental conditions

A K-means algorithm (*vegan* package) was used to classify the sampled stations based on the quality of organic resources using as variables the amount of recalcitrant (C1 + C2) and

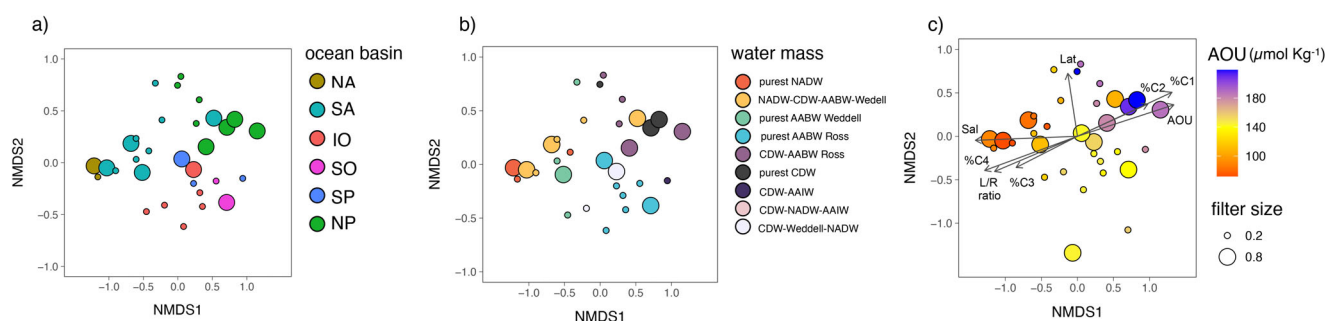


Fig. 1. NMDS ordination of 16S RNA-based communities using Bray–Curtis dissimilarities. Dot size represents the different size fractions: small dots correspond to the 0.2–0.8 μm size fraction, whereas large dots to the 0.8–20 μm size fraction, Dots are colored based on (a) ocean basin (NA: North Atlantic, SA: South Atlantic, IO: Indian Ocean, SO: Southern Ocean, SP: South Pacific, NP: North Pacific), (b) water mass, (c) apparent oxygen utilization (AOU) values. The arrows indicate the environmental conditions that explain best the NMDS ordination patterns (envfit analyses, see “Materials and Methods” section; %C1 and %C2, proportion of the humic like FDOM components; %C3 and %C4, proportion of the protein-like FDOM components; Lat: latitude; ratioLR, labile to recalcitrant FDOM ratio $[(C3 + C4)/(C1 + C2)]$; Sal, salinity).

labile (C3 + C4) fluorescent DOM, and the labile to recalcitrant ratio (L/R ratio), and forcing the partition into three clusters as we wanted to compare the most contrasting conditions. The FDOM characterization of the three clusters of stations can be found in Supplementary Table S2. The clusters comprised waters with high L/R ratios (labile cluster), waters with medium-low L/R ratios (intermediate cluster), and waters with very low L/R ratios (recalcitrant cluster). Pearson correlations between the contribution of the lifestyle categories and the different optical properties of FDOM was performed using the *Hmisc* package (Harrell and Dupont 2016).

Genetic repertoire of prokaryotes with a FL-Is and PA-Is

The functional potential of the different lifestyles was assessed from published metagenomes obtained from the same sampled stations (Acinas et al. 2021, Fig. S1) using the KEGG orthology table retrieved from its companion website (<https://malaspina-public.gitlab.io/malaspina-deep-ocean-microbiome/page/data/>). All the information on how the metagenomes were processed can also be found in that companion website. Functional traits specific to FL-Is and PA-Is prokaryotes were delineated using *CornCob* (see the “Categorization of ASVs in the different lifestyle categories” section for details). The DA approach allows reducing the interpretation bias introduced by the potential presence of prokaryotes of different lifestyle in both size fractions (see “Why differential abundance analyses” section in the Supplementary methods). The KEGG genes (KOs) that did not display any significant DA between the 0.2–0.8 and 0.8–20 μm size fractions were categorized as “shared” since they comprised both core genes shared by the FL-Is and PA-Is categories and genes harbored by dual-Is prokaryotes. Raw functional tables were used for the DA analysis (as *CornCob* requires raw data) and the sub-sampled functional tables of the differentially abundant KOs were used to generate the figures.

We further annotated the metagenomes for carbohydrate-active enzymes (CAZymes) to assess what are the main

differences in the genetic repertoire for carbohydrates utilization of free-living and particle-associated prokaryotes (see Supplementary methods for further information).

Genetic repertoire of prokaryotes inhabiting waters of contrasting OM lability

A differential analysis on the metagenomic data from the stations belonging to the labile and recalcitrant cluster (Fig. 3) was done to assess differences in the metabolic capabilities of communities inhabiting these waters using *CornCob*, as described above. The results of this analysis are compiled in Supplementary Data S2.

Results

Drivers of the active prokaryotic microbiome

The NMDS ordination of RNA-based prokaryotic communities in the bathypelagic did not show a clear segregation between the 0.2–0.8 μm and the 0.8–20 μm size fractions (Fig. 1), and indeed size-fraction explained very little of the total variance in community composition ($\sim 8\%$, PERMANOVA, $p < 0.001$; Supplementary Table S3). Communities from the same ocean basin tended to be more similar than communities from other ocean basins (Fig. 1a), and the same pattern was observed when water masses were considered (Fig. 1b). This geographical ordering of the samples was evident for both size fractions. When considering differences of community composition of all samples (including both size fractions), water masses explained 42% of the variance in community composition, and the ocean basin the samples belonged to 14% (Supplementary Table S3). When both size-fractions were considered separately, the proportion of variance explained by water masses increased to 58% in both size-fractions, whereas the ocean basin explained 18%–19% (Supplementary Table S3).

We then evaluated if the quality of OM and other environmental factors had an imprint in the ordination of the communities (see “Supplementary Methods” section for details on the

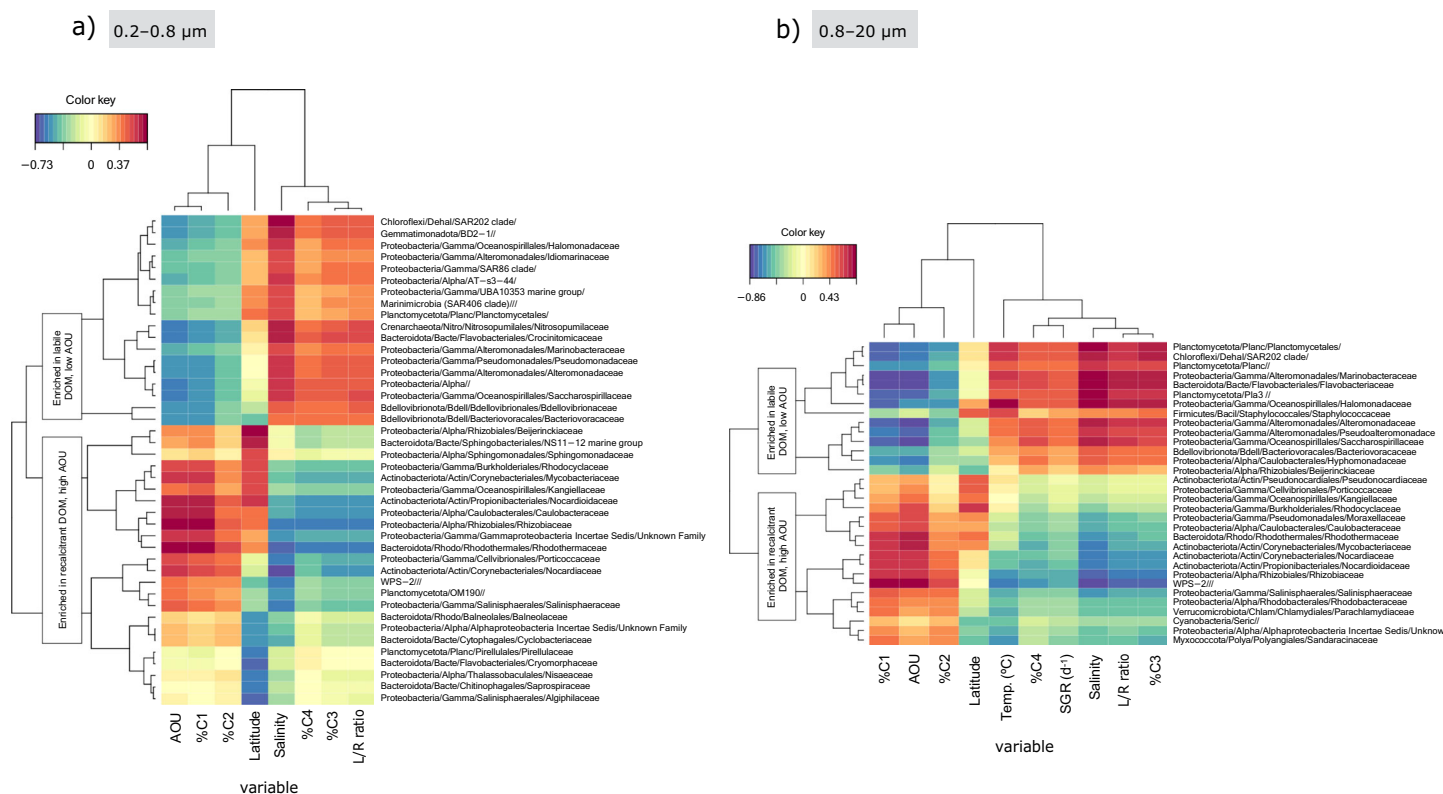


Fig. 2. Pair-wise associations between the relative abundance in the RNA pool of different prokaryotic families and the proportion of the FDOM components, the labile to recalcitrant FDOM ratio and other abiotic and biotic variables (assessed through sPLS analyses, see “Supplementary Methods” section). Only those ASVs that reached 100 sequences in the RNA dataset were considered for the analysis. (a) 0.2–0.8 μm size fraction, (b) 0.8–20 μm size fraction. The color key represents the strength of the positive or negative association. Only associations stronger than 0.5 are shown. %C1 and %C2, proportions of the humic like FDOM components; %C3 and %C4, proportions of the protein-like FDOM components; L/R ratio, labile to recalcitrant FDOM ratio $[\text{C3} + \text{C4}]/[\text{C1} + \text{C2}]$; SGR, specific growth rates).

different variables assessed). We found that latitude, salinity, apparent oxygen utilization (AOU), the proportion of the protein-like FDOM components C3 and C4, the proportion of the humic-like components C1 and C2, and the labile to recalcitrant FDOM ratio were significantly related to the NMDS ordination patterns (Fig. 1c) of both size fractions. AOU represents the amount of oxygen consumed since the last contact of a given water parcel with the atmosphere, and thus integrates respiratory processes and provides an idea of water mass aging (Catalá et al. 2015a). AOU was negatively correlated with the labile to recalcitrant FDOM ratio (Pearson’s $R = -0.58$, $p < 0.05$).

sPLS (see “Supplementary Methods” section) regression analysis identified a subset of prokaryotic families that positively correlated with younger waters (i.e., low AOU) and high labile to recalcitrant FDOM ratio (Fig. 2), which included members of the SAR202, Nitrosopumilaceae, Bdellovibrionota, and Alteromonadales in the 0.2–0.8 μm size fraction, and Planctomycetota, Flavobacteriaceae, and Alteromonadales in the 0.8–20 μm size fraction. These prokaryotic families in the 0.8–20 μm size fraction were also associated with higher specific prokaryotic growth rates (SGR d^{-1} , Fig. 2b). In

contrast, the contribution to the active microbiome of distinct families of Gammaproteobacteria (e.g., Rhodocyclaceae) and Alphaproteobacteria (e.g., Sphingomonadaceae, Rhizobiaceae), and Bacteroidota, in both size fractions, and families of Actinobacteriota in the 0.8–20 μm size fraction, positively correlated with aged waters (i.e., characterized by high AOU) and higher signatures of the humic-like components (lower labile to recalcitrant ratio) (Fig. 2). These results indicate that there is a broad niche partitioning of the active bathypelagic microbiome in both size fractions based on water mass aging and OM characteristics and quality.

Variable contribution of lifestyles to the active bathypelagic prokaryotic microbiome

Next, we explored whether resource availability impacts the contribution of different lifestyles to the active microbiome, delineated using a DA approach (see “Materials and Methods” section). Most ASVs had a dual-ls ($n = 2041$), followed by FL-ls ($n = 867$) and PA-ls ($n = 532$). As expected, FL-ls ASVs generally dominated the 16S DNA sequences of the 0.2–0.8 μm size fraction across stations (range 24%–77%, mean 55%; Supplementary

Fig. S2a) although dual-ls ASVs also presented remarkable contributions (range 13–58, mean 33%). The contribution of FL-ls to the 16S RNA pool of the 0.2–0.8 μm size fraction, however, was much lower (range 4–45%, average 19%; Supplementary Fig. S2a), whereas PA-ls and dual-ls ASVs represented a large fraction of the 16S RNA-based community (up to 85%, on average 33% and 58%, respectively). In the 0.8–20 μm size fraction, PA-ls ASVs were typically the predominant component, accounting for an average 54% in the 16S DNA pool and 60% in the 16S RNA pool, although dual-ls ASVs also accounted for a notable proportion of the sequences.

The taxonomic affiliation of the ASVs of the three lifestyle categories was diverse (Supplementary Fig. S2b). However, in terms of DNA sequences clear differences were observed between the average taxonomic composition of PA-ls and FL-ls categories at the order level, whereas PA-ls and dual-ls assemblages were more similar. FL-ls assemblages in the DNA were largely represented by Crenarchaeota (formerly Thaumarchaeota), SAR324, Chloroflexi (mostly SAR202), Marinimicrobia and Sphingomonadales (Alphaproteobacteria). In contrast, the active free-living microbiome was largely dominated by the Sphingomonadales, which accounted for half of the reads, followed by Chloroflexi (Supplementary Fig. S2b). Total and active PA-ls communities were dominated by Actinobacteriota and different orders of Gammaproteobacteria (Supplementary Fig. S2b). Total and active dual-ls communities were largely composed by several orders of Gammaproteobacteria (Supplementary Fig. S2b) and Alphaproteobacteria (Rhodobacterales and other less abundant orders). Despite the taxonomic composition of PA and dual-ls ASVs appeared similar at the order level, notable differences emerged at the genus level (Supplementary Figs. S3, S4), supporting the idea that the “dual-ls” genuinely exists, and it is not a consequence of a methodological bias in size-fractionation (*see* “Supplementary Methods” section). The taxonomic composition varied considerably within each lifestyle category across stations and size fractions particularly in the active microbiome (Supplementary Figs. S5, S6), suggesting environmental selection of different taxonomic groups.

To assess the contributions of the different lifestyles to the active microbiome in waters with different resource quality we classified the sampled stations according to their FDOM characteristics using a standard *K*-means classification algorithm, forcing the partition into three different clusters that we labeled as labile, intermediate, and recalcitrant (*see* “Materials and Methods” section). Most of the waters sampled were characterized by an intermediate or low L/R ratio (Fig. 3a,b). Although the representation of labile cluster stations was unfortunately low, some trends could be clearly seen among the three clusters. For example, the AOU (Fig. 3b) was significantly higher in the cluster of stations that displayed lower quality of OM (Kruskal–Wallis rank sum test, $p < 0.01$).

PA-ls taxa dominated the active microbiome of the particle-associated (0.8–20 μm) size fraction regardless the OM quality,

as expected (Fig. 3c). However, the contribution of PA-ls taxa to the active microbiome in the 0.2–0.8 μm size fraction remarkably increased with the lability of OM (Pearson’s $R = 0.66$, $p < 0.05$), representing $\sim 70\%$ of the RNA-based community in stations classified within the labile cluster and less than 20% in the recalcitrant cluster. In contrast, FL-ls ASVs represented up to 40% of the RNA pool in waters depleted of labile OM, and together with dual-ls taxa accounted for most of the active microbiome in these waters (Fig. 3c).

Insights into the potential physiology of the different lifestyles

Following (Salter et al. 2015; Kirchman 2016; Lankiewicz et al. 2016) we used RNA–DNA relationships to estimate the metabolic activity (or growth rates) of the different lifestyle categories. There was an overall positive correlation between the amount of RNA and DNA sequences of individual ASVs belonging to each of the lifestyle categories, but the relationship was weak (Supplementary Fig. S7). The slope of the RNA–DNA relationship of the ASVs belonging to the FL-ls category (1.1, $R^2 = 0.46$) was significantly lower than the slopes for the dual-ls and PA-ls categories (1.86, $R^2 = 0.41$, 1.74, $R^2 = 0.42$, respectively, no overlapping 95% confidence interval of the model II Major Axis regression slopes, 10,000 permutations; Supplementary Fig. S7). This suggests comparatively lower metabolic activity of FL-ls taxa than taxa with a dual-ls or PA-ls.

To further assess differences in the genomic repertoire of the contrasted lifestyles we used a DA approach on the metagenomic data available from the same stations (Fig. S1). This allowed us to explore untargeted differences in the global functional repertoire of the different lifestyles, beyond the analyses done previously (Acinas et al. 2021) that mainly focused on key biogeochemical markers. Since we could not differentiate between the core genes and genes harbored by dual-ls taxa, we focused only in the differences in the functional capabilities of FL-ls and PA-ls prokaryotes (*see* “Materials and Methods” section for further details).

The most striking differences in the gene repertoire of FL-ls and PA-ls taxa were the contrasting number of genes devoted to environmental and genetic information processing (Fig. 4). PA-ls genetic content included a high number of genes coding for two-component systems, substrate binding proteins and permeases that were not detected in the FL-ls gene repertoire (Supplementary Fig. S8). FL-ls prokaryotes, in contrast, contained a large number of genes involved in genetic information processing that were not detected in the PA-ls prokaryotes (Fig. 4a,b; Supplementary Data S1), and genes that code for proteases. FL-ls communities also displayed a relatively higher number of genes involved in energy metabolism (Fig. 4a,b) such as genes coding for a V-type ATPase and the *nuo* genes (Supplementary Fig. S9), which encode a Type I (energy-conserving) NADH dehydrogenase (Archer and Elliott 1995). Genes involved in carbon fixation were shared between both lifestyle categories (Supplementary Fig. S9).

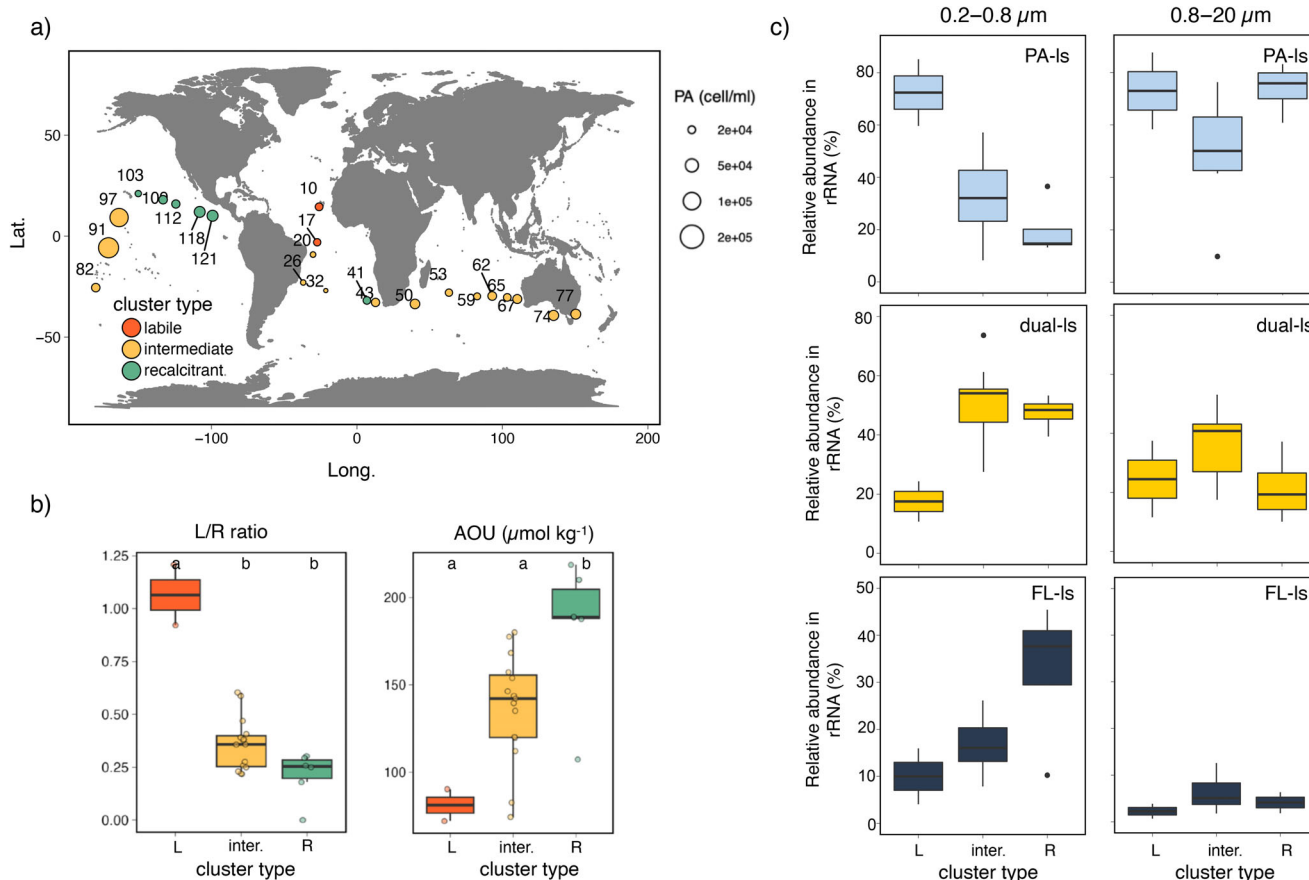


Fig. 3. Varying contribution of FL-Is, dual-Is, and PA-Is to the active prokaryotic microbiome in waters with different organic matter quality. *K*-means clustering of stations based on the FDOM characteristics and the L/R FDOM ratio. **(a)** Map showing the distribution of the stations colored by the cluster they belong to: labile (high values of L/R ratio, see Supplementary Table S2 for details), intermediate and recalcitrant (low values of L/R ratio). The size of the dots represents the prokaryotic abundance in each of the stations. **(b)** Boxplots showing the variation of the L/R FDOM ratio and the AOU, which integrates respiratory processes, in the labile (L), intermediate (inter.) and recalcitrant (R) cluster of stations. Different letters above the boxplots indicate significant differences among clusters (Kruskal–Wallis and post hoc Dunn test, $p < 0.05$). **(c)** Percent contribution of the different lifestyle categories to the rRNA in each of the cluster types, in both size fractions.

Furthermore, genes involved in the synthesis of most vitamins, particularly of vitamins B5, B7, and B12, were found in FL-Is communities, but not in PA-Is communities, indicating that PA-Is prokaryotes are not generally able to synthesize these vitamins and likely obtain them from the particles or from the FL-Is communities (Supplementary Fig. S10a). This is supported by the observation that vitamin B7 (Biotin) and B12 transporters were significantly enriched in PA-Is communities (Supplementary Fig. S8). We found that the capability to synthesize different B vitamins was widely distributed within FL-Is taxa (Supplementary Fig. S10b). Besides a broad array of transporters (Supplementary Fig. S8), PA-Is taxa harbored Type II secretion systems (T2SS). PA-Is taxa also differed from FL-Is taxa in the abundance of genes involved in cell motility, metabolism of lipids and secondary metabolites (Fig. 4a,b). In relation to carbohydrate metabolism, PA-Is taxa had a number of genes that were not present in the FL-Is communities (Fig. 4a,b; Supplementary Fig. S11).

The role of resources quality in shaping the function of bathypelagic communities was further explored by looking at the genomic repertoire of prokaryotes inhabiting waters of contrasting OM quality (Supplementary Fig. S12; Data S2). Genes devoted to cell motility were more abundant in communities from the labile cluster and significantly decreased towards waters enriched in recalcitrant material (Fig. 4c), in both size-fractions. The most differentially abundant gene for environmental processing in the communities in the labile cluster was *uhpB* (K07675) (Supplementary Fig. S12), which controls the expression of sugar transporters (Wright et al. 2000). In contrast, in the metagenomes of the recalcitrant cluster other transport systems were abundant, such as a TRAP-transporter (K11688) and different intermembrane transporters (e.g., K10016, K05847, K02067).

The carbohydrate metabolism of PA-Is and FL-Is prokaryotes was additionally examined by looking at their contrasting genetic repertoire in terms of carbohydrate-active enzymes

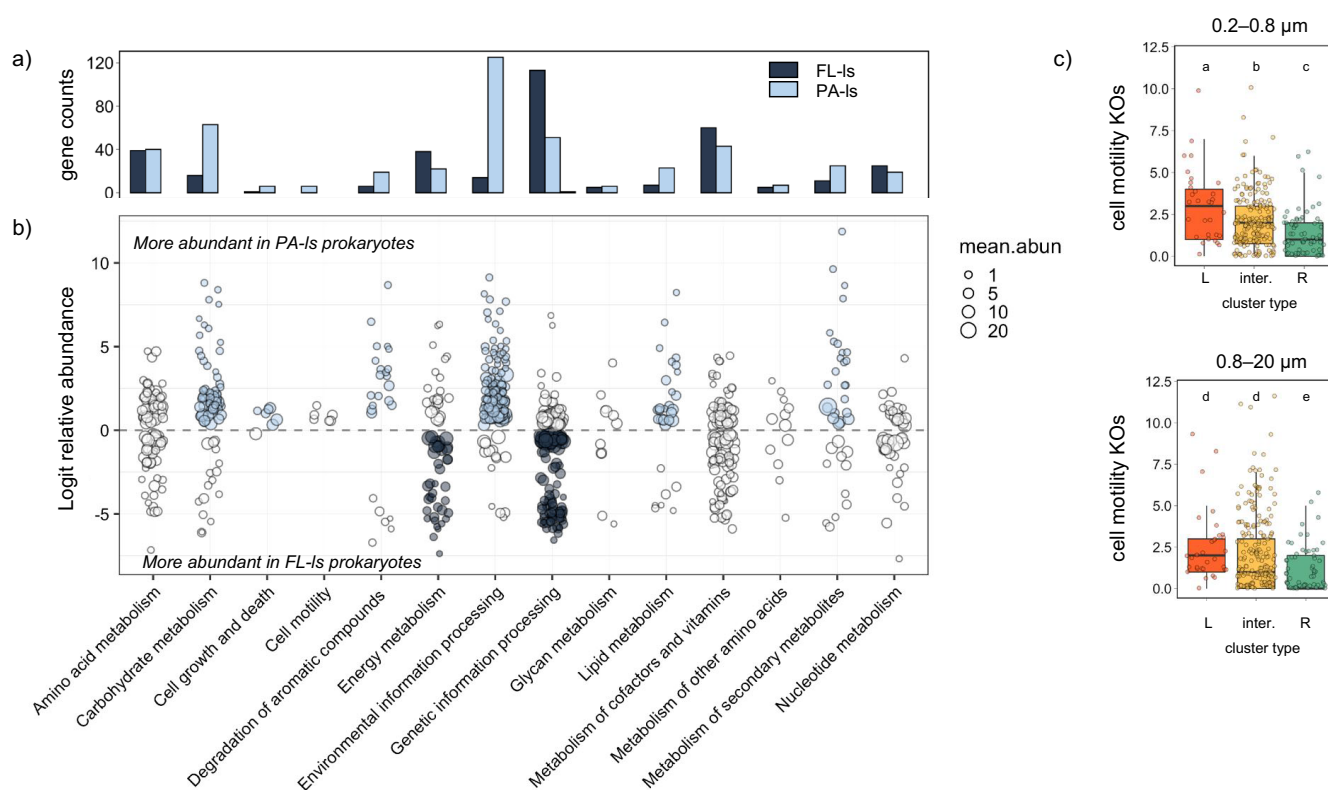


Fig. 4. Functional characterization of differentially abundant genes (based on KO annotations) between metagenomes from the 0.2 to 0.8 μm size fraction and metagenomes from the 0.8 to 20 μm size fraction. **(a)** number of KOs belonging to each of the functional categories that are differentially found in both size fractions. **(b)** Details of the DA tests for each size fraction. Each circle represents a differentially abundant KO. Positive values imply that a KO was more abundant in the 0.8–20 μm size fraction (i.e., PA-Is KOs), whereas negative values indicate that the KO was more abundant in the 0.2–0.8 μm size fraction (i.e., FL-Is KOs). Circle size represents the mean relative abundance of each KO in the bathypelagic samples. Color of circles highlight those functional categories that were clearly enriched in either the FL-Is or the PA-Is prokaryotes (i.e., the number of KOs in a given size fraction were 1.5X the ones detected in the other size fraction). **(c)** Abundance of cell motility KOs in the metagenomes from the labile and recalcitrant clusters defined in Fig. 3. Different letters above the boxplots indicate significant differences among clusters (Kruskal–Wallis and post hoc Dunn test, $p < 0.05$).

(CAZymes), which are involved in the cleaving of carbohydrates. Out of 274 CAZyme families, we found 78 and 32 families that were significantly enriched in the particle-attached (0.8–20 μm) and in the free-living fraction (0.2–0.8 μm), respectively (Supplementary Data S3). There was a differential enrichment of CAZymes belonging to different families but the largest differences were found in the number of glycosyl transferases, which were overrepresented in the 0.8–20 μm size fraction (Fig. 5a). These enzymes are involved in the synthesis of extracellular polysaccharides (Bi et al. 2015) that are crucial in cellular adhesion, retaining enzymes and other molecules. There were also notable differences in the number and abundance of different families of glycoside hydrolases (Fig. 5a, see Supplementary results for further details). Differences in auxiliary activity enzymes that have ligninolytic activity or are involved in redox reactions in conjunction with other CAZymes, as well as differences in carbon esterases were also observed (Fig. 5a). The richness of CAZymes was similar in both size-fractions, but the abundance was comparatively higher in the 0.8–20 μm size fraction (Fig. 5b). However, we

found that younger waters comparatively enriched in labile material displayed lower richness of CAZymes than waters with more recalcitrant FDOM (Fig. 5c). Yet, this observation should be taken with caution given the low number of stations categorized as labile (Fig. 3a).

The differences in the metabolic profiles of prokaryotic communities inhabiting waters with different OM quality were further confirmed by means of Biolog GN2 plates[®]. We found that communities from waters depleted of labile OM displayed comparatively higher capability to utilize complex carbon sources than communities from waters with more labile material (Supplementary Fig. S13, see Table S4 for the list of substrates within each category).

Discussion

Water mass aging and the quality of OM determine the structure of active bathypelagic communities

A strong linkage was found between the active bathypelagic microbiome structure, water mass aging and resource

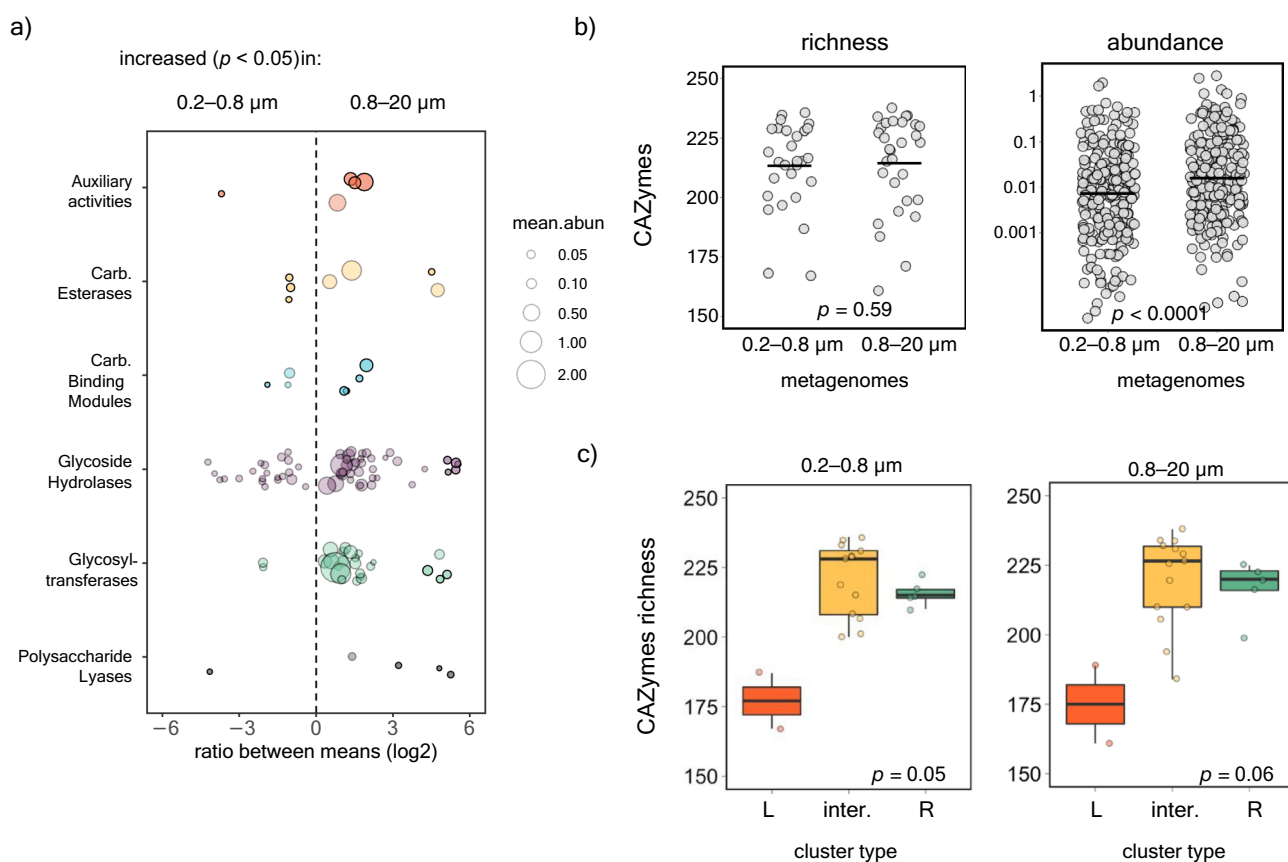


Fig. 5. Carbohydrate active enzymes (CAZymes) in bathypelagic metagenomes. **(a)** Log₂-transformed ratio of mean per genome abundance of CAZymes between the 0.8–20 and 0.2–0.8 μm metagenomes (only those with significantly different abundances after Wilcoxon rank sum test, $p < 0.05$, are plotted). **(b)** CAZY families richness and per genome abundance in the 0.2–0.8 and 0.8–20 μm metagenomes. The solid line indicates the mean, the p -value of the Wilcoxon rank sum test is also shown. **(c)** Boxplots depicting the richness of CAZymes in the different FDOM clusters (see fig. 3 for details) for both size fractions. The p -value of the Kruskal–Wallis test is shown.

quality in both size fractions, as shown by the NMDS ordination of the samples (Fig. 1) and the niche partitioning of the different prokaryotic families (Fig. 2). The observed imprint of water mass aging in the 0.8–20 μm size-fraction suggests that particles from aged waters have gone through different remineralization and transport histories compared to those from younger waters, likely resulting in differing biochemical composition.

The lack of segregation of the 16S RNA-based communities based on size fraction in the non-metric multidimensional scaling (Fig. 1) contrasts with the clear separation previously observed in the DNA (Salazar et al. 2016). This indicates that the composition of the active microbiome in both size-fractions is more similar than when considering the total microbiome.

Groups like Nitrosopumilaceae appeared associated with younger waters with a higher proportion of FDOM labile components (Fig. 2), which would be somehow counterintuitive given their potential for chemolithotrophy (Könneke et al. 2005). However, they rely on the oxidation of ammonia as source of energy to fix inorganic carbon, and this reduced compound is also released through particle solubilization. Despite SAR202

bacteria known ability to use recalcitrant organic compounds (Landry et al. 2017; Liu et al. 2020), they did not appear associated with the aged water masses enriched in recalcitrant DOM (Fig. 2). This suggests that other factors like microbial interactions, or extra carbon or energy, play a role in controlling the activity of this prokaryotic group. Indeed, SAR202 cells have also been shown to actively participate in amino acid consumption in deep waters using single-cell approaches (Varela et al. 2008), suggesting they can benefit from both labile and recalcitrant compounds. The fact that the contribution of Alteromonadales to the RNA pool was positively associated with an increasing proportion of labile FDOM components in both size fractions, along with higher specific growth rates (SGR d⁻¹) in the 0.8–20 μm size-fraction (Fig. 2), aligns with previous findings showing that Alteromonadales play a pivotal role in processing labile DOM (Pedler et al. 2014), respond swiftly to organic carbon inputs in the water column (Pelve et al. 2017) and display fast growth rates in the ocean (Kirchman 2016). RNA sequences of Actinobacterial families were associated to aged water masses enriched in recalcitrant DOM, which agrees with the view that this phylum can

utilize a broad spectrum of refractory compounds (Chen et al. 2016). Other families associated to these aged water masses may be able to use various electron acceptors to degrade aromatic compounds, as reported in the Gammaproteobacteria Rhodocyclaceae (Oren 2014) that appeared linked to the recalcitrant FDOM.

The contribution of different lifestyles to the active microbiome varies along resource availability gradients

Our DA analyses of ASVs abundances showed varying contribution of the FL-ls, PA-ls, and dual-ls to both size fractions across the global ocean. The dual-ls has been so far mostly overlooked, but its substantial contribution to both size fractions suggests that dual-ls prokaryotes are able to thrive on particles but also in the free-living realm. This category was largely composed by genera that were not present in the PA-ls category, such as *Marinobacter* and *Idiomarina* (Supplementary Fig. S3), which have been detected in sediment traps material (Preston et al. 2020; Poff et al. 2021) as well as free-living (Sebastián et al. 2019), in agreement with a dual-ls. The dominance of both PA-ls and dual-ls ASVs in the RNA-based community of both size fractions (Supplementary Fig. S2) likely accounts for the lack of segregation between the two fractions observed in Fig. 1. Particle-associated taxa, along with some genera detected in the dual-ls taxa (Supplementary Fig. S3), include copiotrophic taxa (Ivars-Martinez et al. 2008; Lauro et al. 2009). These bacteria are known for their high ribosomal content (Lankiewicz et al. 2016), which likely allows them to swiftly respond to the presence of particles or resource patches. This may explain why PA-ls and dual-ls dominated the RNA pool also in the 0.2–0.8 μm size fraction.

The important contribution of PA-ls taxa to the RNA pool of the 0.2–0.8 μm size fraction ($\sim 70\%$) in the stations with better quality of OM (Fig. 3), suggests that detached PA-ls taxa get stimulated by the plume of labile OM produced during particle remineralization (Kjørboe and Jackson 2001). In contrast, despite their presumably lower metabolic rates (Supplementary Fig. S7), FL-ls ASVs made up to 40% of the RNA-based communities in waters depleted of labile OM, and together with dual-ls taxa, they dominated the active microbiome in the free-living realm (Fig. 3). Given the scarcity of particles in the bathypelagic, prokaryotes associated with particles are typically believed to comprise less than 10% of the total (volumetric) prokaryotic abundance (Mével et al. 2008; Zhang et al. 2020). If these estimates hold true, taxa with dual-ls and FL-ls would notably contribute to global bathypelagic metabolism, particularly in aged water masses enriched with recalcitrant organic material. A major contributor to the RNA pool of the FL-ls assemblages was the Alphaproteobacteria Sphingomonadales (Supplementary Figs. S2, S6), which are known for their growth in oligotrophic marine waters and their ability to use recalcitrant compounds (Miller et al. 2010; Kertész et al. 2018). These bacteria seem to cope well with extended periods without fresh

organic carbon, as in an experiment where bathypelagic communities received no external organic carbon input they represented up to a third of the RNA-based prokaryotic community during the initial 5 months (Sebastián et al. 2018; Supplementary Fig. S14). Based on our results, Sphingomonadales could play a substantial role in carbon processing in vast areas of the bathypelagic ocean.

Contrasting genetic repertoire of the different lifestyles and functional biogeography of the bathypelagic microbiome

The differential genomic content of PA and FL taxa offered further insight into the metabolic strategies of these lifestyles. One remarkable feature is the prevalence of two-component systems in PA-taxa, which has also been recently reported in sinking-particle-associated bacteria (Leu et al. 2022). These regulatory systems are regarded as the principal mechanism for signal transduction in bacteria, enabling cells to sense and respond to changes in environmental cues (Alm et al. 2006). Low numbers of two-component systems have been reported in streamlined genomes (Alm et al. 2006), and in the sunlit ocean the limited presence of these genes has been considered a distinctive feature of an oligotrophic lifestyle (Held et al. 2019). The comparatively lower number of two-component systems in FL-ls prokaryotes implies they have a limited capability to regulate gene expression in response to environmental variation, suggesting FL-ls taxa are bathypelagic oligotrophs with a relatively uniform metabolism regardless of the external environmental cues, similar to what has been described for dominant oligotrophs in the surface ocean (e.g., SAR11 bacteria [Giovannoni 2017]). This aligns with our finding that FL-ls taxa displayed on average significantly lower RNA:DNA values than dual-ls and PA-ls taxa (Supplementary Fig. S7), which is another typical feature of oligotrophs (Lankiewicz et al. 2016). FL-ls taxa, in contrast, harbored many genetic information processing genes that were not present in the PA-ls taxa, some genes coding for proteases, which degrade intracellular proteins and have a role in stress responses (Hilt and Wolf 1996), some energy conserving mechanisms, and vitamin synthesis genes. It is known that members of Crenarchaeota, which were numerically important members of the FL-ls communities (Supplementary Fig. S2b), encode and express biosynthetic pathways for several B vitamins (Santoro et al. 2015), and release some of these vitamins as a by-product of their metabolism (Bayer et al. 2019). Yet the ability to synthesize different B vitamins was taxonomically widespread (Supplementary Fig. S10b), indicating that different FL-ls prokaryotes may play a crucial role in supplying B vitamins for bathypelagic metabolism.

Genes for particle colonization (such as T2SS (Nivaskumar and Francetic 2014), and glycosyltransferases (Bi et al. 2015) for the biofilm formation on the particles, and cell motility genes) were enriched in the PA-ls genetic repertoire, as well as many other genes involved in carbohydrate metabolism (Figs. 4, 5; Supplementary Fig. S11; Data S2). Some of these genes are

related to glycogen metabolism (GH77, GH13, and CMB48), which is known to play a key role in survival and adaptation to fluctuating carbon supply (Sekar et al. 2020). The decrease in the abundance of cell-motility genes in the aged waters (Fig. 4c) was consistent with the drop in the contribution of PA-Is ASVs to the active microbiome in these waters (Fig. 3c). Being motile is crucial to swim towards nutrient patches or particles (Lambert et al. 2019), particularly in the bathypelagic realm where these hotspots are scarce, although some non-motile prokaryotes may also colonize particles after encountering them by chance (Słomka et al. 2020). Prokaryotes from older waters displayed more energy-conserving mechanisms than those from younger waters (Supplementary Fig. S12), reinforcing the view that these waters received comparatively lower inputs of fresh organic carbon.

OM quality also influenced the CAZymes repertoire of the communities. The greater richness of CAZymes found in waters enriched in recalcitrant OM (Fig. 5c) suggests a certain degree of diversification in the substrate use capabilities of these communities, in agreement with the hypothesis that recalcitrant DOM is composed by a myriad of diverse diluted compounds (Arrieta et al. 2015). Although more studies are needed to confirm this given the low number of stations in the labile cluster, the observation of higher polymer use capabilities in communities from the aged waters adds some support to this potential diversification. The ratio of complex carbon sources to carbohydrate utilization was also higher in the aged water masses enriched in recalcitrant DOM, in line with the observed increase in the ratio of polymer to carbohydrate utilization from the surface to the deep ocean (Sala et al. 2020) following the increase in the recalcitrant nature of the DOM (Catalá et al. 2015b).

Our work provides compelling evidence that there is a regionalization of the prokaryotic microbiome in the deep waters of the tropical and subtropical ocean. We demonstrate that there is a fraction of prokaryotic communities thriving as free-living organisms and well adapted to scarce labile OM availability. These prokaryotes include both putative slow growers that have a FL-Is and limited metabolic flexibility to respond to environmental changes, and dual-Is taxa, which are potentially capable of fast growth and also able to cope with low carbon inputs, perhaps by using various terminal electron acceptors, as reported for other marine opportunistic taxa (Singer et al. 2011). The contribution of these FL-Is and dual-Is taxa to the active microbiome increases when the availability of labile OM decreases, the conditions prevailing in the global bathypelagic desert. These findings are supported by our observation that waters depleted of labile OM have functionally distinct communities, with apparently less ability to colonize particles, and higher ability to use complex-carbon sources than communities inhabiting waters with comparatively higher proportions of labile OM.

Particles in the bathypelagic realm are scarce, except during episodes of elevated carbon flux (Smith et al. 2018; Poff et al. 2021), as most sinking particles are remineralized within

the mesopelagic (Herndl and Reinthaler 2013). Thus, obligate and optional free-living prokaryotes may have a previously overlooked role in bathypelagic metabolism, which could have strong implications for its functioning.

Data availability statement

All data generated or analyzed during this study are included in this article (and its supplementary information files) or it is publicly available. All 16S raw sequences used in this study are publicly available at the European Nucleotide Archive (ENA, <https://www.ebi.ac.uk/ena/browser/home>) under Study accession numbers SRP031469 and SRP079340 for the DNA and RNA datasets, respectively. The metagenomic raw sequences are publicly available at both DOE's JGI Integrated Microbial Genomes and Microbiomes (IMG/MER) and the ENA. Individual metagenome assemblies, annotation files, and alignment files can be accessed at IMG/MER. All accession numbers are listed in Acinas et al. 2021 (Supplementary Data S1). The environmental metadata used in this study are provided in Supplementary Data S4.

References

- Acinas, S. G., and others. 2021. Deep ocean metagenomes provide insight into the metabolic architecture of bathypelagic microbial communities. *Commun. Biol.* **4**: 604. doi:10.1038/s42003-021-02112-2
- Alm, E., K. Huang, and A. Arkin. 2006. The evolution of two-component systems in bacteria reveals different strategies for niche adaptation. *PLoS Comput. Biol.* **2**: e143. doi:10.1371/journal.pcbi.0020143
- Archer, C. D., and T. Elliott. 1995. Transcriptional control of the *nuo* operon which encodes the energy-conserving NADH dehydrogenase of *Salmonella typhimurium*. *J. Bacteriol.* **177**: 2335–2342. doi:10.1128/jb.177.9.2335-2342.1995
- Aristegui, J., S. Agustí, J. J. Middelburg, and C. M. Duarte. 2005. Respiration in the mesopelagic and bathypelagic zones of the oceans, p. 181–205. *In* P. Del Giorgio and P. Williams [eds.], *Respiration in aquatic ecosystems*. Oxford Univ. Press.
- Aristegui, J., J. M. Gasol, C. M. Duarte, and G. J. Herndl. 2009. Microbial oceanography of the dark ocean's pelagic realm. *Limnol. Oceanogr.* **54**: 1501–1529. doi:10.4319/lo.2009.54.5.1501
- Arrieta, J. M., E. Mayol, R. L. Hansman, G. J. Herndl, T. Dittmar, and C. M. Duarte. 2015. Dilution limits dissolved organic carbon utilization in the deep ocean. *Science* **348**: 331–333. doi:10.1126/science.1258955
- Baltar, F., J. Aristegui, J. M. Gasol, E. Sintes, and G. J. Herndl. 2009a. Evidence of prokaryotic metabolism on suspended particulate organic matter in the dark waters of the subtropical North Atlantic. *Limnol. Oceanogr.* **54**: 182–193. doi:10.4319/lo.2009.54.1.0182

- Baltar, F., J. Arístegui, E. Sintés, H. M. Van Aken, J. M. Gasol, and G. J. Herndl. 2009b. Prokaryotic extracellular enzymatic activity in relation to biomass production and respiration in the meso- and bathypelagic waters of the (sub) tropical Atlantic. *Environ. Microbiol.* **11**: 1998–2014. doi:[10.1111/j.1462-2920.2009.01922.x](https://doi.org/10.1111/j.1462-2920.2009.01922.x)
- Bayer, B., and others. 2019. Ammonia-oxidizing archaea release a suite of organic compounds potentially fueling prokaryotic heterotrophy in the ocean. *Environ. Microbiol.* **21**: 4062–4075. doi:[10.1111/1462-2920.14755](https://doi.org/10.1111/1462-2920.14755)
- Bergauer, K., A. Fernandez-Guerra, J. A. L. Garcia, R. R. Sprenger, R. Stepanauskas, M. G. Pachiadaki, O. N. Jensen, and G. J. Herndl. 2018. Organic matter processing by microbial communities throughout the Atlantic water column as revealed by metaproteomics. *Proc. Natl. Acad. Sci. USA* **115**: E400–E408. doi:[10.1073/pnas.1708779115](https://doi.org/10.1073/pnas.1708779115)
- Bi, Y., C. Hubbard, P. Purushotham, and J. Zimmer. 2015. Insights into the structure and function of membrane-integrated processive glycosyltransferases. *Curr. Opin. Struct. Biol.* **34**: 78–86. doi:[10.1016/j.sbi.2015.07.008](https://doi.org/10.1016/j.sbi.2015.07.008)
- Callahan, B. J., P. J. McMurdie, M. J. Rosen, A. W. Han, A. J. A. Johnson, and S. P. Holmes. 2016. DADA2: High-resolution sample inference from Illumina amplicon data. *Nat. Methods* **13**: 581–583. doi:[10.1038/nmeth.3869](https://doi.org/10.1038/nmeth.3869)
- Carr, N., C. E. Davis, S. Blackbird, L. R. Daniels, C. Preece, M. Woodward, and C. Mahaffey. 2019. Seasonal and spatial variability in the optical characteristics of DOM in a temperate shelf sea. *Prog. Oceanogr.* **177**: 101929. doi:[10.1016/j.pocean.2018.02.025](https://doi.org/10.1016/j.pocean.2018.02.025)
- Catalá, T. S., and others. 2015a. Water mass age and aging driving chromophoric dissolved organic matter in the dark global ocean. *Global Biogeochem. Cycl.* **29**: 917–934. doi:[10.1002/2014GB005048](https://doi.org/10.1002/2014GB005048)
- Catalá, T. S., and others. 2015b. Turnover time of fluorescent dissolved organic matter in the dark global ocean. *Nat. Commun.* **6**: 5986. doi:[10.1038/ncomms6986](https://doi.org/10.1038/ncomms6986)
- Chen, P., and others. 2016. Diversity, biogeography, and biodegradation potential of actinobacteria in the deep-sea sediments along the southwest Indian ridge. *Front. Microbiol.* **7**: 1340. doi:[10.3389/fmicb.2016.01340](https://doi.org/10.3389/fmicb.2016.01340)
- Cottrell, M. T., and D. L. Kirchman. 2016. Transcriptional control in marine copiotrophic and oligotrophic bacteria with streamlined genomes. *Appl. Environ. Microbiol.* **82**: 6010–6018. doi:[10.1128/AEM.01299-16](https://doi.org/10.1128/AEM.01299-16)
- DeLong, E. F., and others. 2006. Community genomics among stratified microbial assemblages in the ocean's interior. *Science* **311**: 496–503. doi:[10.1126/science.1120250](https://doi.org/10.1126/science.1120250)
- Devresse, Q., K. W. Becker, A. F. Dilmahamod, E. Ortega-Retuerta, and A. Engel. 2023. Dissolved organic matter fluorescence as a tracer of upwelling and microbial activities in two cyclonic eddies in the eastern tropical North Atlantic. *J. Geophys. Res. Oceans* **128**: 1–24. doi:[10.1029/2023JC019821](https://doi.org/10.1029/2023JC019821)
- Giovannoni, S. J. 2017. SAR11 bacteria: The most abundant plankton in the oceans. *Ann. Rev. Mar. Sci.* **9**: 231–255. doi:[10.1146/annurev-marine-010814-015934](https://doi.org/10.1146/annurev-marine-010814-015934)
- Hansell, D. A., C. A. Carlson, D. J. Repeta, and R. Schlitzer. 2009. Dissolved organic matter in the ocean: A controversy stimulates new insights. *Oceanography* **22**: 202–211. doi:[10.5670/oceanog.2009.109](https://doi.org/10.5670/oceanog.2009.109)
- Harrell, F. E., and C. Dupont. 2016. Package “Hmisc”: Harrell miscellaneous. R Top. Doc. <https://CRAN.R-project.org/package=Hmisc>
- Held, N. A., M. R. McIlvin, D. M. Moran, M. T. Laub, and M. A. Saito. 2019. Unique patterns and biogeochemical relevance of two-component sensing in marine bacteria. *mSystems* **4**: e00317-18. doi:[10.1128/mSystems.00317-18](https://doi.org/10.1128/mSystems.00317-18)
- Hernández-León, S., and others. 2020. Large deep-sea zooplankton biomass mirrors primary production in the global ocean. *Nat. Commun.* **11**: 6048. doi:[10.1038/s41467-020-19875-7](https://doi.org/10.1038/s41467-020-19875-7)
- Herndl, G. J., and T. Reinthaler. 2013. Microbial control of the dark end of the biological pump. *Nat. Geosci.* **6**: 718–724. doi:[10.1038/ngeo1921](https://doi.org/10.1038/ngeo1921)
- Hilt, W., and D. H. Wolf. 1996. Proteasomes: Destruction as a programme. *Trends Biochem. Sci.* **21**: 96–102. doi:[10.1016/S0968-0004\(96\)10012-8](https://doi.org/10.1016/S0968-0004(96)10012-8)
- Ivars-Martinez, E., A. B. Martin-Cuadrado, G. D'Auria, A. Mira, S. Ferreria, J. Johnson, R. Friedman, and F. Rodriguez-Valera. 2008. Comparative genomics of two ecotypes of the marine planktonic copiotroph *Alteromonas macleodii* suggests alternative lifestyles associated with different kinds of particulate organic matter. *ISME J.* **2**: 1194–1212. doi:[10.1038/ismej.2008.74](https://doi.org/10.1038/ismej.2008.74)
- Jørgensen, L., C. A. Stedmon, T. Kragh, S. Markager, M. Middelboe, and M. Søndergaard. 2011. Global trends in the fluorescence characteristics and distribution of marine dissolved organic matter. *Mar. Chem.* **126**: 139–148. doi:[10.1016/j.marchem.2011.05.002](https://doi.org/10.1016/j.marchem.2011.05.002)
- Jørgensen, L., C. A. Stedmon, M. A. Granskog, and M. Middelboe. 2014. Tracing the long-term microbial production of recalcitrant fluorescent dissolved organic matter in seawater. *Geophys. Res. Lett.* **41**: 2481–2488. doi:[10.1002/2014GL059428](https://doi.org/10.1002/2014GL059428)
- Kertesz, M. A., A. Kawasaki, and A. Stolz. 2018. Aerobic hydrocarbon-degrading Alphaproteobacteria: Sphingomonadales, p. 1–21. *In* T. J. McGenity [ed.], Taxonomy, genomics and ecophysiology of hydrocarbon-degrading microbes. Springer International Publishing.
- Kjørboe, T., and G. A. Jackson. 2001. Marine snow, organic solute plumes, and optimal chemosensory behavior of bacteria. *Limnol. Oceanogr.* **46**: 1309–1318. doi:[10.4319/lo.2001.46.6.1309](https://doi.org/10.4319/lo.2001.46.6.1309)
- Kirchman, D. L. 2016. Growth rates of microbes in the oceans. *Ann. Rev. Mar. Sci.* **8**: 285–309. doi:[10.1146/annurev-marine-122414-033938](https://doi.org/10.1146/annurev-marine-122414-033938)

- Könneke, M., A. E. Bernhard, J. R. de la Torre, C. B. Walker, J. B. Waterbury, and D. A. Stahl. 2005. Isolation of an autotrophic ammonia-oxidizing marine archaeon. *Nature* **437**: 543–546. doi:10.1038/nature03911
- Lambert, B. S., V. I. Fernandez, and R. Stocker. 2019. Motility drives bacterial encounter with particles responsible for carbon export throughout the ocean. *Limnol. Oceanogr. Lett.* **4**: 113–118. doi:10.1002/lol2.10113
- Landry, Z., B. K. Swan, G. J. Herndl, R. Stepanauskas, and S. J. Giovannoni. 2017. SAR202 genomes from the dark ocean predict pathways for the oxidation of recalcitrant dissolved organic matter. *mBio* **8**: e00413–e00417. doi:10.1128/mBio.00413-17
- Lankiewicz, T. S., M. T. Cottrell, and D. L. Kirchman. 2016. Growth rates and rRNA content of four marine bacteria in pure cultures and in the Delaware estuary. *ISME J.* **10**: 823–832. doi:10.1038/ismej.2015.156
- Lauro, F. M., and others. 2009. The genomic basis of trophic strategy in marine bacteria. *Proc. Natl. Acad. Sci. USA* **106**: 15527–15533. doi:10.1073/pnas.0903507106
- Leu, A. O., J. M. Eppley, A. Burger, and E. F. DeLong. 2022. Diverse genomic traits differentiate sinking-particle-associated versus free-living microbes throughout the oligotrophic open ocean water column. *mBio* **13**: e0156922. doi:10.1128/mbio.01569-22
- Liu, S., R. Parsons, K. Opalk, and others. 2020. Different carboxyl-rich alicyclic molecules proxy compounds select distinct bacterioplankton for oxidation of dissolved organic matter in the mesopelagic Sargasso Sea. *Limnol. Oceanogr.* **65**: 1532–1553. doi:10.1002/lno.11405
- Martin, B. D., D. Witten, and A. D. Willis. 2020. Modeling microbial abundances and dysbiosis with beta-binomial regression. *Ann. Appl. Stat.* **14**: 94–115. doi:10.1214/19-AOAS1283
- Mével, G., M. Vernet, M. Goutx, and J. F. Ghiglione. 2008. Seasonal to hour variation scales in abundance and production of total and particle-attached bacteria in the open NW Mediterranean Sea (0–1000 m). *Biogeosciences* **5**: 1573–1586. doi:10.5194/bg-5-1573-2008
- Miller, T. R., A. L. Delcher, S. L. Salzberg, E. Saunders, J. C. Detter, and R. U. Halden. 2010. Genome sequence of the dioxin-mineralizing bacterium *Sphingomonas wittichii* RW1. *J. Bacteriol.* **192**: 6101–6102. doi:10.1128/JB.01030-10
- Nelson, N. B., and D. A. Siegel. 2013. The global distribution and dynamics of chromophoric dissolved organic matter. *Ann. Rev. Mar. Sci.* **5**: 447–476. doi:10.1146/annurev-marine-120710-100751
- Nivaskumar, M., and O. Francetic. 2014. Type II secretion system: A magic beanstalk or a protein escalator. *Biochim. Biophys. Acta Mol. Cell Res.* **1843**: 1568–1577. doi:10.1016/j.bbamcr.2013.12.020
- Oksanen, J., F. G. Blanchet, R. Kindt, and others. 2015. Vegan: Community Ecology Package. R package version 2.5-5. R Packag. version.
- Oren, A. 2014. The family Rhodocyclaceae, p. 975–998. In E. Rosenberg, E. F. DeLong, S. Lory, E. Stackebrandt, and F. Thompson [eds.], *The prokaryotes*. Springer.
- Pedler, B. E., L. I. Aluwihare, and F. Azam. 2014. Single bacterial strain capable of significant contribution to carbon cycling in the surface ocean. *Proc. Natl. Acad. Sci. USA* **111**: 7202–7207. doi:10.1073/pnas.1401887111
- Pelve, E. A., K. M. Fontanez, and E. F. DeLong. 2017. Bacterial succession on sinking particles in the ocean's interior. *Front. Microbiol.* **8**. doi:10.3389/fmicb.2017.02269
- Poff, K. E., A. O. Leu, J. M. Eppley, D. M. Karl, and E. F. DeLong. 2021. Microbial dynamics of elevated carbon flux in the open ocean's abyss. *Proc. Natl. Acad. Sci. USA* **118**: e2018269118. doi:10.1073/pnas.2018269118
- Preston, C. M., C. A. Durkin, and K. M. Yamahara. 2020. DNA metabarcoding reveals organisms contributing to particulate matter flux to abyssal depths in the North East Pacific Ocean. *Deep Sea Res. II Top. Stud. Oceanogr.* **173**: 104708. doi:10.1016/j.dsr2.2019.104708
- Reinthal, T., H. M. van Aken, and G. J. Herndl. 2010. Major contribution of autotrophy to microbial carbon cycling in the deep North Atlantic's interior. *Deep Sea Res. II Top. Stud. Oceanogr.* **57**: 1572–1580. doi:10.1016/j.dsr2.2010.02.023
- Ruiz-González, C., and others. 2020. Major imprint of surface plankton on deep ocean prokaryotic structure and activity. *Mol. Ecol.* **29**: 1820–1838. doi:10.1111/mec.15454
- Sala, M. M., and others. 2020. Prokaryotic capability to use organic substrates across the global tropical and subtropical ocean. *Front. Microbiol.* **11**. doi:10.3389/fmicb.2020.00918
- Salazar, G., F. M. Cornejo-Castillo, V. Benítez-Barríos, E. Fraile-Nuez, X. A. Álvarez-Salgado, C. M. Duarte, J. M. Gasol, and S. G. Acinas. 2016. Global diversity and biogeography of deep-sea pelagic prokaryotes. *ISME J.* **10**: 596–608. doi:10.1038/ismej.2015.137
- Salazar, G., F. M. Cornejo-Castillo, E. Borrull, and others. 2015. Particle-association lifestyle is a phylogenetically conserved trait in bathypelagic prokaryotes. *Mol. Ecol.* **24**: 5692–5706. doi:10.1111/mec.13419
- Salter, I., P. E. Galand, S. K. Fagervold, P. Lebaron, I. Obernosterer, M. J. Oliver, M. T. Suzuki, and C. Tricoire. 2015. Seasonal dynamics of active SAR11 ecotypes in the oligotrophic Northwest Mediterranean Sea. *ISME J.* **9**: 347–360. doi:10.1038/ismej.2014.129
- Santoro, A. E., C. L. Dupont, R. A. Richter, and others. 2015. Genomic and proteomic characterization of “*Candidatus Nitrosopelagicus brevis*”: An ammonia-oxidizing archaeon from the open ocean. *Proc. Natl. Acad. Sci. USA* **112**: 1173–1178. doi:10.1073/pnas.1416223112
- Sebastián, M., J.-C. Auguet, C. X. Restrepo-Ortiz, M. M. Sala, C. Marrasé, and J. M. Gasol. 2018. Deep ocean prokaryotic communities are remarkably malleable when facing long-

- term starvation. *Environ. Microbiol.* **20**: 713–723. doi:[10.1111/1462-2920.14002](https://doi.org/10.1111/1462-2920.14002)
- Sebastián, M., M. Estrany, C. Ruiz-González, I. Forn, M. M. Sala, J. M. Gasol, and C. Marrasé. 2019. High growth potential of long-term starved deep ocean opportunistic heterotrophic bacteria. *Front. Microbiol.* **10**. doi:[10.3389/fmicb.2019.00760](https://doi.org/10.3389/fmicb.2019.00760)
- Sekar, K., S. M. Linker, J. Nguyen, A. Grünhagen, R. Stocker, and U. Sauer. 2020. Bacterial glycogen provides short-term benefits in changing environments. *Appl. Environ. Microbiol.* **86**. doi:[10.1128/AEM.00049-20](https://doi.org/10.1128/AEM.00049-20)
- Singer, E., E. A. Webb, W. C. Nelson, J. F. Heidelberg, N. Ivanova, A. Pati, and K. J. Edwards. 2011. Genomic potential of *Marinobacter aquaeolei*, a biogeochemical “opportunitroph”. *Appl. Environ. Microbiol.* **77**: 2763–2771. doi:[10.1128/AEM.01866-10](https://doi.org/10.1128/AEM.01866-10)
- Stomka, J., U. Alcolombri, E. Secchi, R. Stocker, and V. I. Fernandez. 2020. Encounter rates between bacteria and small sinking particles. *New J. Phys.* **22**: 043016. doi:[10.1088/1367-2630/ab73c9](https://doi.org/10.1088/1367-2630/ab73c9)
- Smith, K. L., H. A. Ruhl, C. L. Huffard, M. Messié, and M. Kahru. 2018. Episodic organic carbon fluxes from surface ocean to abyssal depths during long-term monitoring in NE Pacific. *Proc. Natl. Acad. Sci. USA* **115**: 12235–12240. doi:[10.1073/pnas.1814559115](https://doi.org/10.1073/pnas.1814559115)
- Sohrin, R., M. Isaji, Y. Obara, S. Agostini, Y. Suzuki, Y. Hiroe, T. Ichikawa, and K. Hidaka. 2011. Distribution of *Synechococcus* in the dark ocean. *Aquat. Microb. Ecol.* **64**: 1–14. doi:[10.3354/ame01508](https://doi.org/10.3354/ame01508)
- Swan, B. K., and others. 2011. Potential for chemolithoautotrophy among ubiquitous bacteria lineages in the dark ocean. *Science* **333**: 1296–1300. doi:[10.1126/science.1203690](https://doi.org/10.1126/science.1203690)
- Tang, K., Y. Yang, D. Lin, S. Li, W. Zhou, Y. Han, K. Liu, and N. Jiao. 2016. Genomic, physiologic, and proteomic insights into metabolic versatility in *Roseobacter clade* bacteria isolated from deep-sea water. *Sci. Rep.* **6**: 35528. doi:[10.1038/srep35528](https://doi.org/10.1038/srep35528)
- Varela, M. M., H. M. van Aken, and G. J. Herndl. 2008. Abundance and activity of *Chloroflexi*-type SAR202 bacterioplankton in the meso- and bathypelagic waters of the (sub)tropical Atlantic. *Environ. Microbiol.* **10**: 1903–1911. doi:[10.1111/j.1462-2920.2008.01627.x](https://doi.org/10.1111/j.1462-2920.2008.01627.x)
- Wright, J. S., I. N. Olekhnovich, G. Touchie, and R. J. Kadner. 2000. The histidine kinase domain of UhpB inhibits UhpA action at the *Escherichia coli* uhpT promoter. *J. Bacteriol.* **182**: 6279–6286. doi:[10.1128/JB.182.22.6279-6286.2000](https://doi.org/10.1128/JB.182.22.6279-6286.2000)
- Yamashita, Y., and E. Tanoue. 2008. Production of bio-refractory fluorescent dissolved organic matter in the ocean interior. *Nat. Geosci.* **1**: 579–582. doi:[10.1038/ngeo279](https://doi.org/10.1038/ngeo279)
- Zhang, Y., H. Jing, and X. Peng. 2020. Vertical shifts of particle-attached and free-living prokaryotes in the water column above the cold seeps of the South China Sea. *Mar. Pollut. Bull.* **156**: 111230. doi:[10.1016/j.marpolbul.2020.111230](https://doi.org/10.1016/j.marpolbul.2020.111230)
- Zhao, Z., F. Baltar, and G. J. Herndl. 2020. Linking extracellular enzymes to phylogeny indicates a predominantly particle-associated lifestyle of deep-sea prokaryotes. *Sci. Adv.* **6**: eaaz4354. doi:[10.1126/sciadv.aaz4354](https://doi.org/10.1126/sciadv.aaz4354)

Acknowledgments

This research was funded by the Spanish Ministry of Economy and Competitiveness Science and Innovation through the Consolider-Ingenio programme (project Malaspina 2010 Expedition, ref. CSD2008-00077). We thank F.M. Cornejo-Castillo, E. Borrull, C. Díez-Vives, E. Lara, and D. Vaqué for their help in sampling. We also thank our fellow scientists and the crew and chief scientists of the different cruise legs for the smooth operation. Sequencing at the JGI was supported by US Department of Energy (DOE) JGI 2011 Microbes Program grant CSP 387 to S.G.A. The work conducted by the US Department of Energy Joint Genome Institute is supported by the Office of Science of the US Department of Energy under contract no. DE-AC02-05CH11231. Additional funding was provided by Spanish Ministry of Economy and Competitiveness grants MAGGY (CTM2017-87736-R), MALASPINOMICS (CTM2011-15461-E), DOREMI (CTM2012-34294), ANIMA (CTM2015-65720-R), MIAU (RTI2018-101025-B-I00). GS held a Ph.D. JAE-Predoc (CSIC). This work has been carried out with the institutional support of the “Severo Ochoa Centre of Excellence” accreditation (CEX2019-000928-S). We thank Clara Ruiz-González, Francisco M Cornejo-Castillo and Mar Benavides for their useful comments on a previous version of the manuscript.

Conflict of Interest

None declared.

Submitted 18 May 2023

Revised 06 October 2023

Accepted 28 December 2023

Associate editor: Hans-Peter Grossart